

Supplementary Information for

Self-Organizing Properties of Triethylsilylethynyl-Anthradithiophene on Monolayer Graphene Electrodes in Solution-Processed Transistors

Jaeyoung Jang,^{‡a} Jaesung Park,^{‡b,c} Sooji Nam,^a John E. Anthony,^d Youngsoo Kim,^e Keun Soo Kim,^f Kwang S. Kim,^{*b} Byung Hee Hong,^{*c} and Chan Eon Park^{*a}

^a Polymer Research Institute, Department of Chemical Engineering, Pohang University of Science and Technology (POSTECH), Pohang, 790-784 (Rep. Korea). Fax: +82-52-279-8298; Tel: +82-54-279-2269; E-mail: cep@postech.ac.kr

^b Center for Superfunctional Materials, Department of Chemistry, Pohang University of Science and Technology (POSTECH), Pohang, 790-784, Korea. kim@postech.ac.kr

^c Department of Chemistry, Seoul National University, Seoul, 151-747, Korea. byunghee@snu.ac.kr

^d Department of Chemistry, University of Kentucky, Lexington, Kentucky, 40506, USA

^e Department of Physics, Seoul National University, Seoul, 151-747, Korea

^f Department of Physics and Graphene Research Institute, Sejong University, Seoul, 143-747, Korea

‡ These authors contributed equally to this work.

* Corresponding Author

* e-mail: cep@postech.ac.kr; kim@postech.ac.kr; byunghee@snu.ac.kr

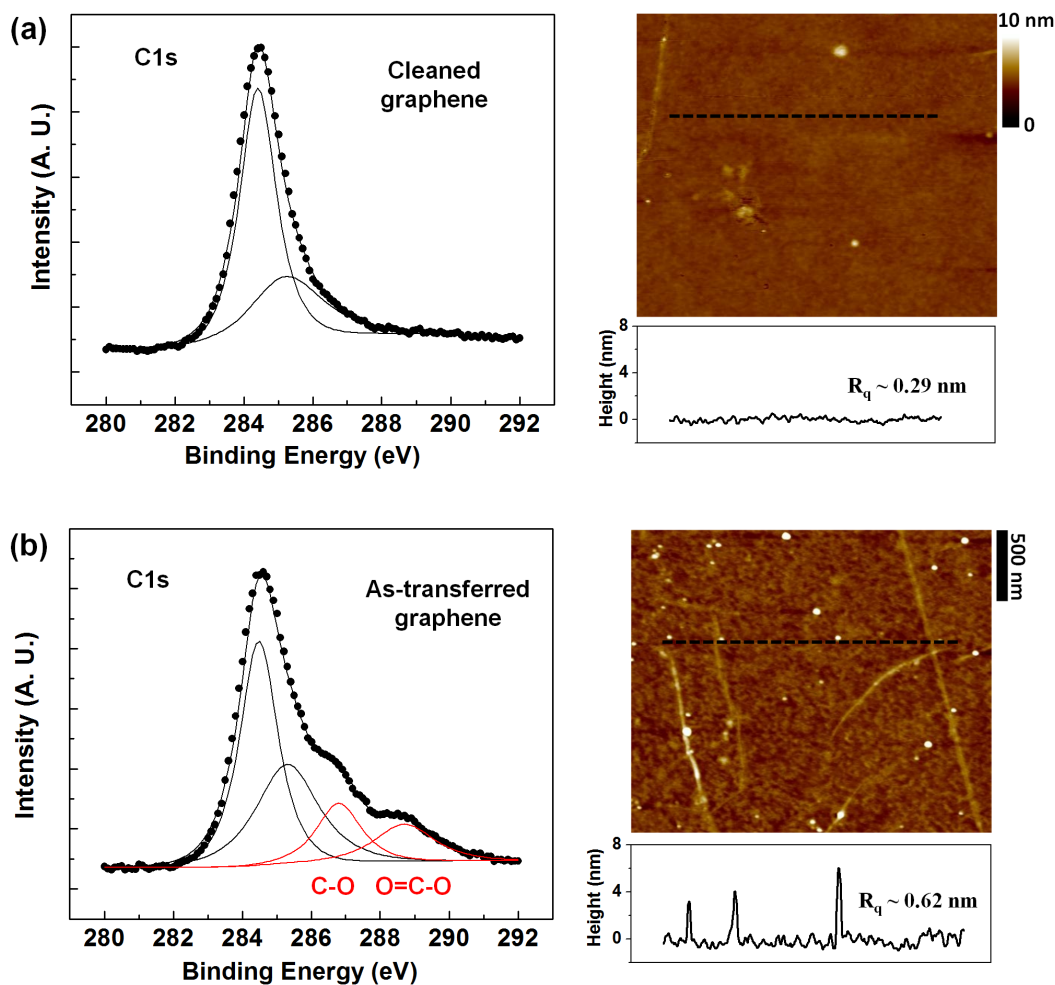


Fig. S1. X-ray photoelectron spectroscopy (XPS) C1s spectra (left), AFM topographs (right and top) and the height profiles (right and bottom) of the cleaned (a) and as-transferred graphene (b) films.

The XPS spectra for the as-transferred graphene surface displayed peaks corresponding to C-O and O=C-O bonds (red lines), indicating the presence of PMMA residue carbonyl functional groups on the graphene surface.¹ No peaks corresponding to oxygen-containing groups were observed in the spectra of the cleaned graphene, suggesting the effective removal of PMMA residue after the removal process.

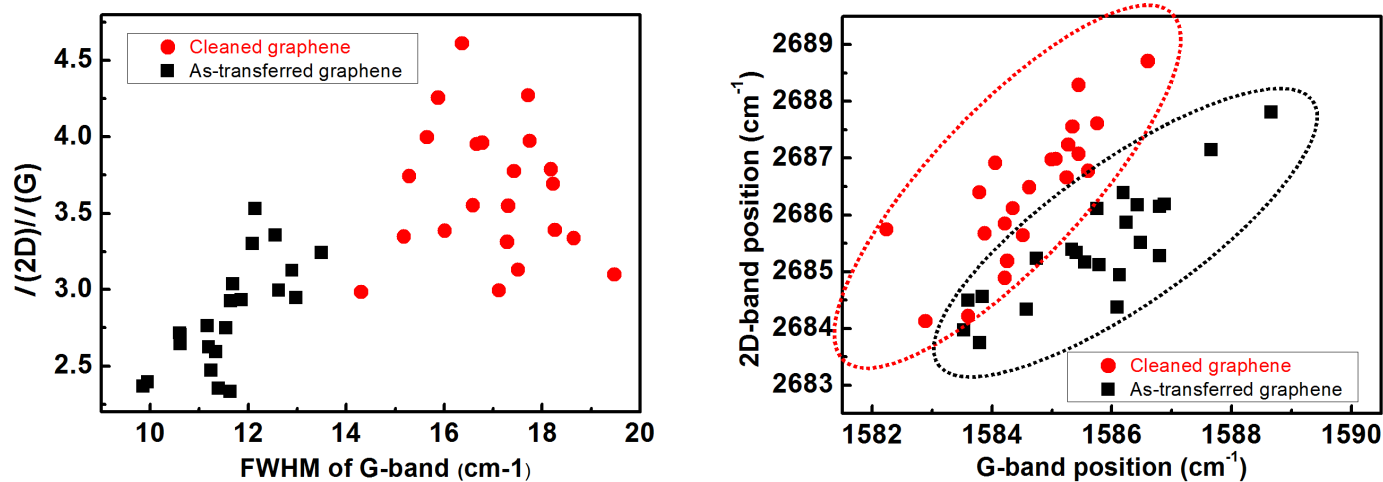


Fig. S2. I_{2D}/I_G versus FWHM of G-band (left) and 2D-band position versus G-band position (right) for the cleaned (red circles) and as-transferred (black squares) monolayer graphene on SiO_2/Si substrates.

The separated statistical distributions extracted from Raman spectra between as-transferred and cleaned graphene samples clearly show the effect of our residue-removal process. The origin of the variation in each separated region might be due to the factors affecting Raman spectra, such as the stain and charge inhomogeneity of graphene, and the substrate flatness.²

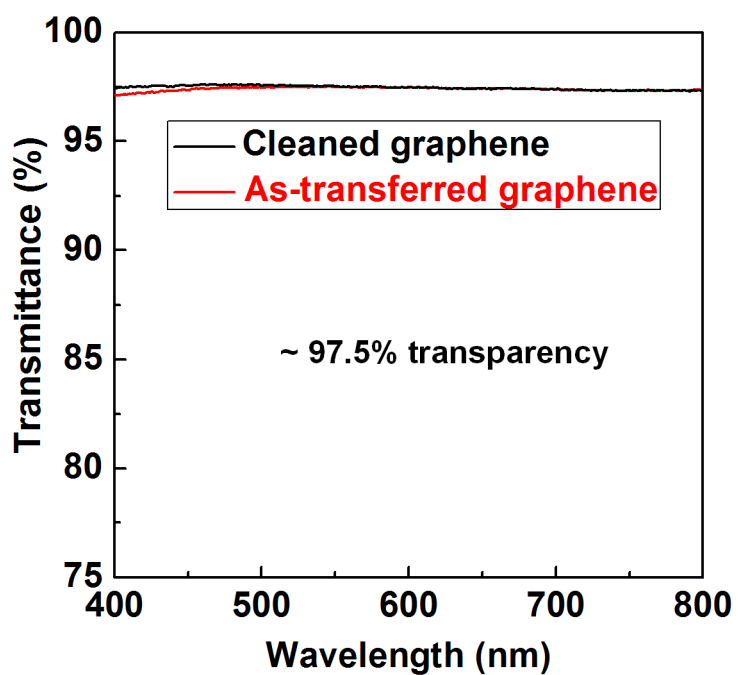


Fig. S3. UV-Vis spectra of the cleaned and as-transferred graphene films. The high transparency of more than 97.5% was attributed to the monolayer thickness of the graphene films.

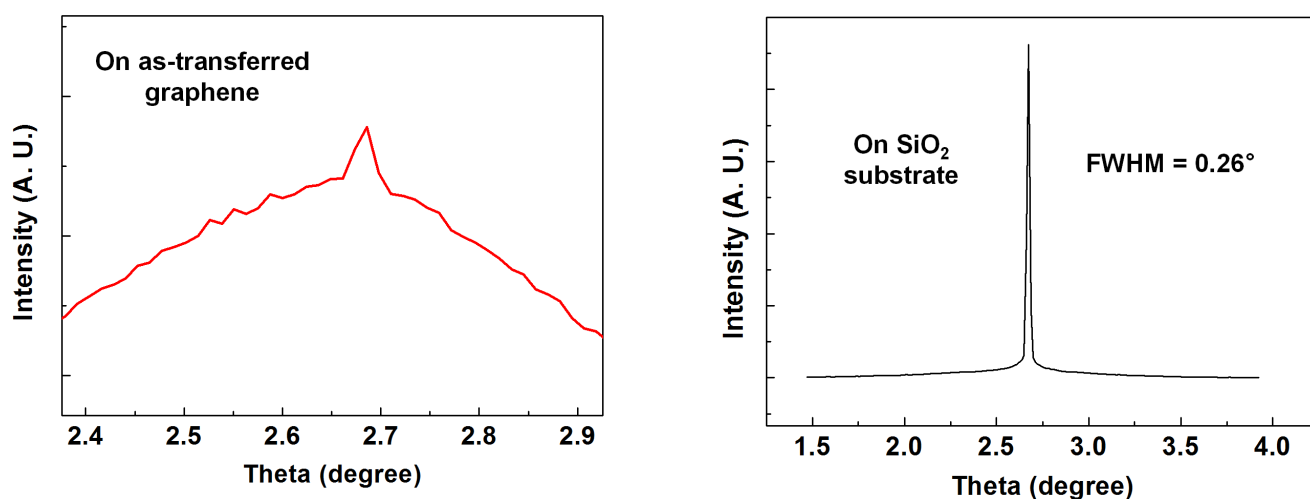


Fig. S4. Enlarged view of the rocking curve for TES-ADT thin films formed on as-transferred graphene films (left). Tilted crystalline domains in the out-of-plane direction were dominant (broad peaks) and the surface-normal domains were less prevalent (small sharp peaks). Rocking curve for TES-ADT thin films prepared on a SiO₂ substrate (right).

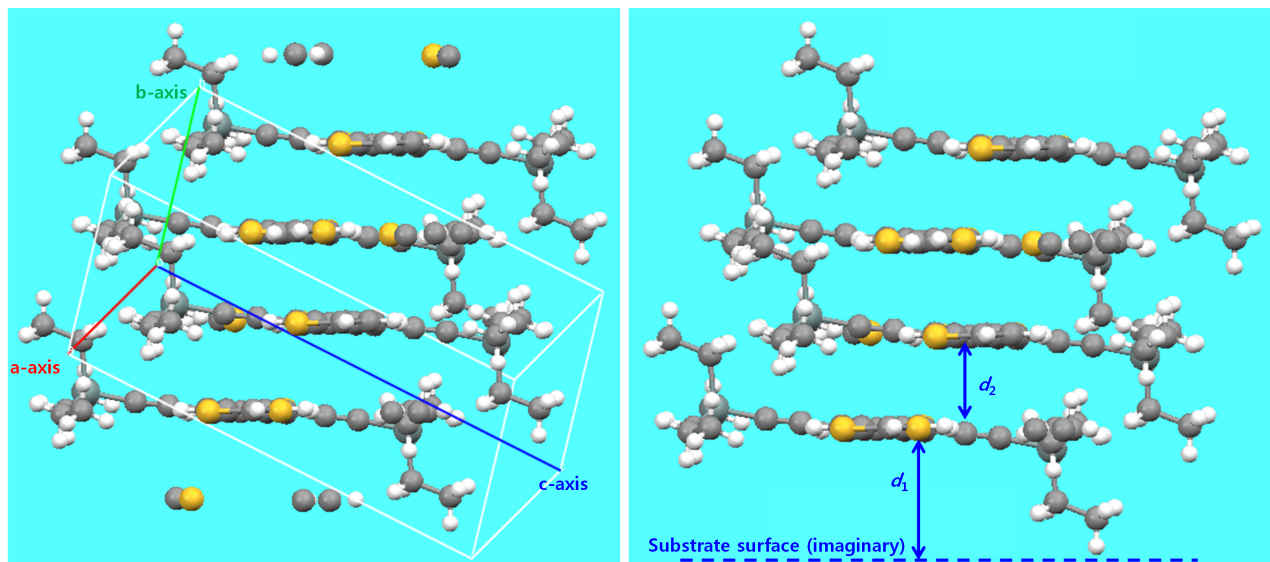


Fig. S5. Molecular packing pattern of TES-ADT with (left) and without (right) unit cell axis (left) (CIF file from the reference [3]).

Figure S5 shows one possible packing pattern of TES-ADT on graphene surface in case of stacking *via* lying-down molecular assembly. As illustrated in the right image, we can infer that lying-down molecular assembly is avoided because d_1 is much larger than d_2 .

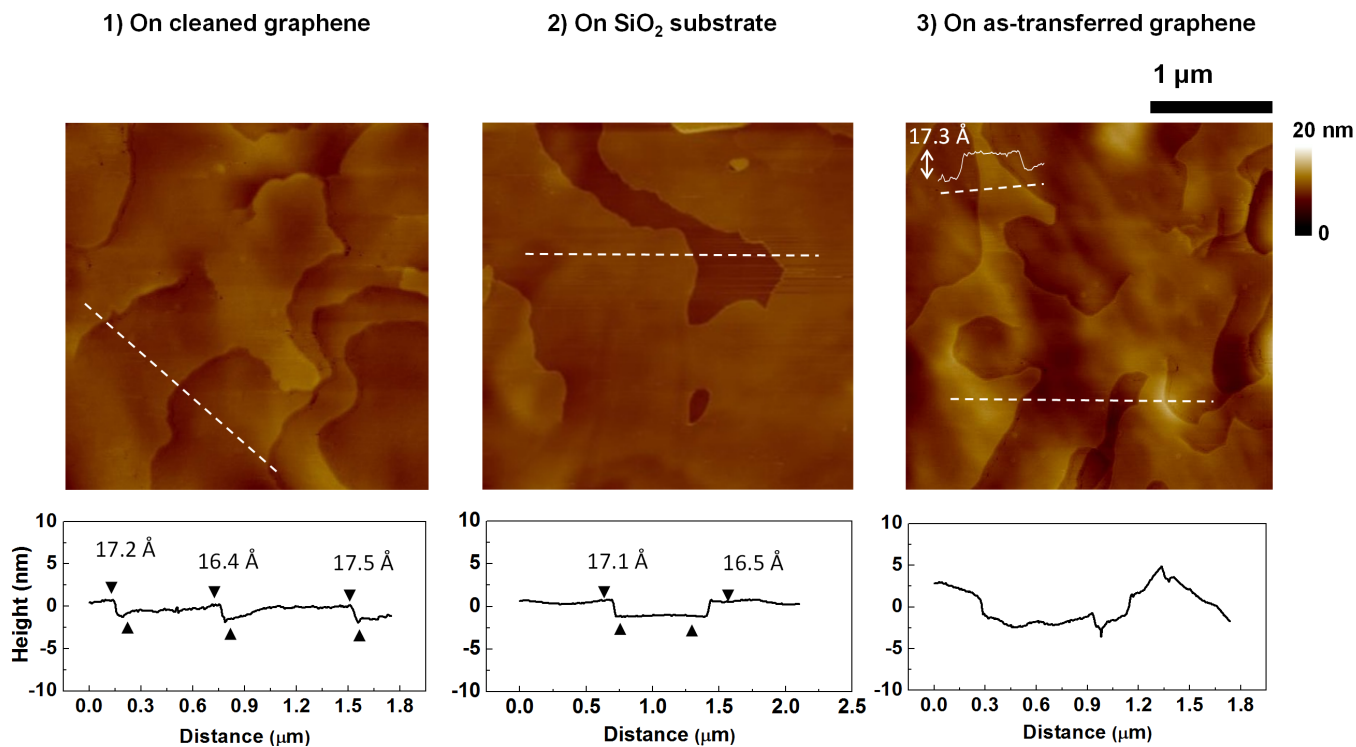


Fig. S6. AFM topographs and height profiles for solvent-vapor annealed TES-ADT thin films formed on cleaned/as-transferred graphene films or a SiO₂ substrate. The white dotted lines correspond to the cross-sectional height profiles shown below each topograph.

The surfaces of the TES-ADT films grown on the cleaned graphene mainly displayed a flat terrace morphology with a regular step height that coincided with the *c*-axis length of the TES-ADT (16.7 Å), similar to the films grown on the SiO₂ substrate. On the other hand, the TES-ADT thin films grown on as-transferred graphene were characterized by a morphology in which the height of each tile matched the *c*-axis length of the TES-ADT (see the inset cross-sectional height profile in the AFM image), but the overall film morphology appeared uneven and somewhat wavy. These morphological features agreed well with the experimental XRD study results.

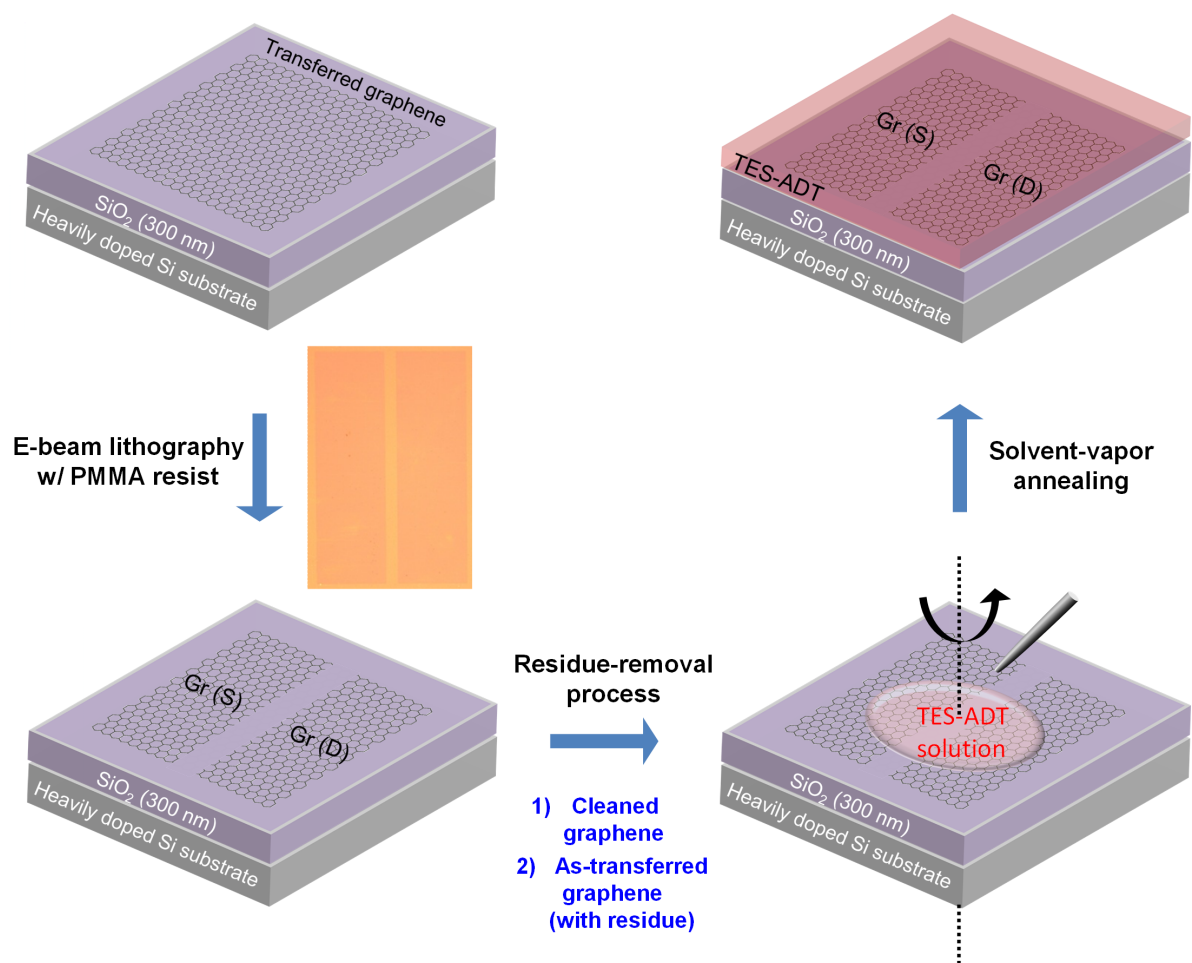


Fig. S7. Schematic illustration of the experimental procedure used for device fabrication. An optical microscopy image shows the defined graphene S/D electrodes.

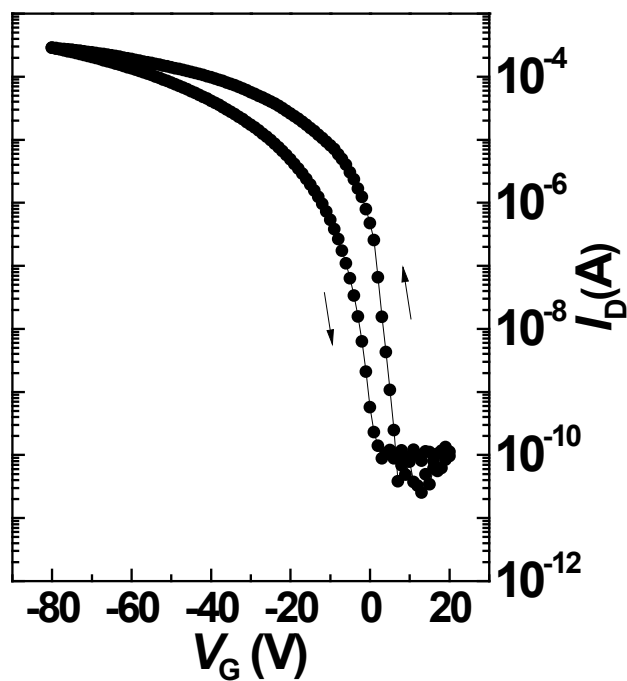


Fig. S8. Transfer characteristics of TES-ADT FET using cleaned graphene electrodes for forward (20V to -80V) and reverse (-80V to 20V) gate voltage sweeps. Small hysteresis indicates good electrical stability of the TES-ADT FETs using cleaned graphene electrodes.

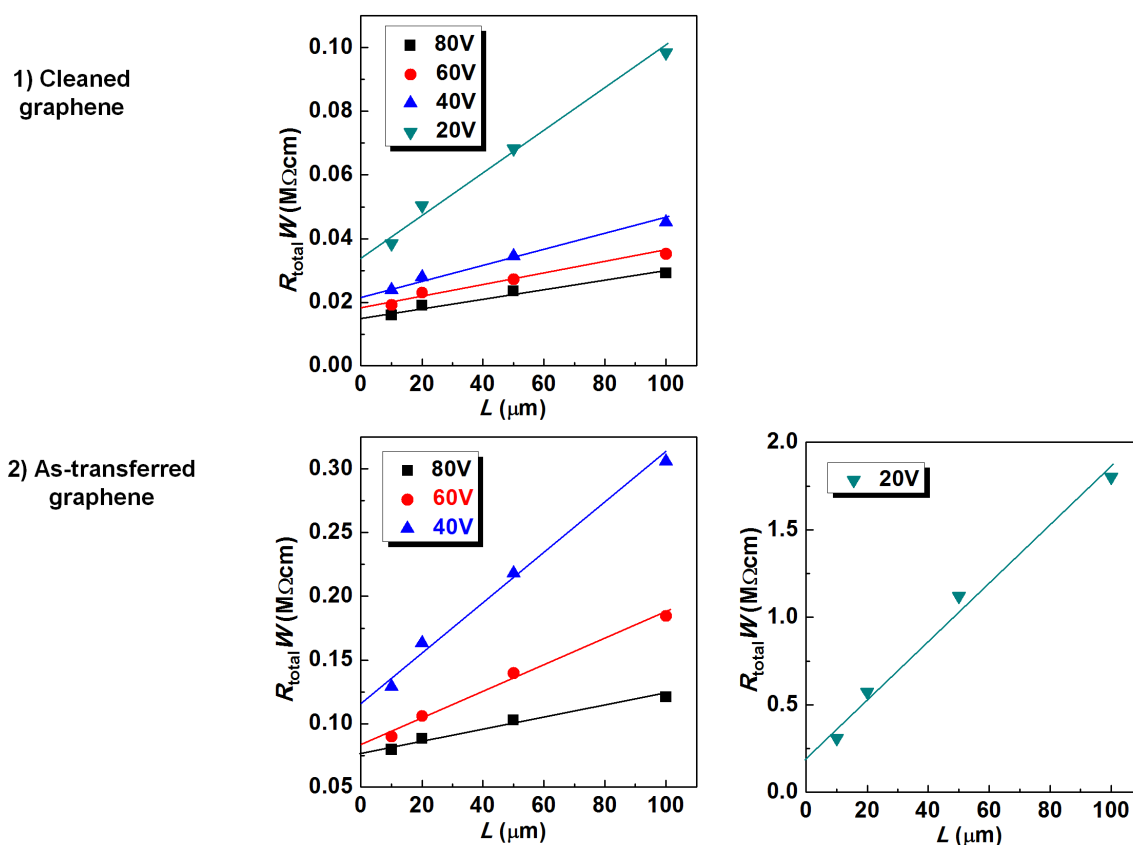


Fig. S9. Channel width-normalized total resistance (R_{total}) for the TES-ADT OFETs prepared with graphene S/D electrodes, as a function of the V_G values. The 20 V values for the as-transferred graphene devices were significantly larger than the other values and, therefore, are plotted separately to facilitate comparison.

R_{total} was obtained from the inverse slope of the I - V curve for each device (for a W of 1000 μm and L values of 10, 20, 50, or 100 μm) in the linear regime at each gate voltage. The contact resistance (R_c) was obtained from the following equation:

$$R_{\text{total}} = R_c + R_{\text{ch}} = R_c + \frac{L}{WC_i \mu_i (V_G - V_{T,i})}$$

where R_{ch} , μ_i , and $V_{T,i}$ are the channel resistance, intrinsic field-effect mobility, and intrinsic threshold voltage, respectively.⁴ In other words, the $L = 0$ intercept of the linear extrapolation based on the experimental data provides an approximate value of R_c .

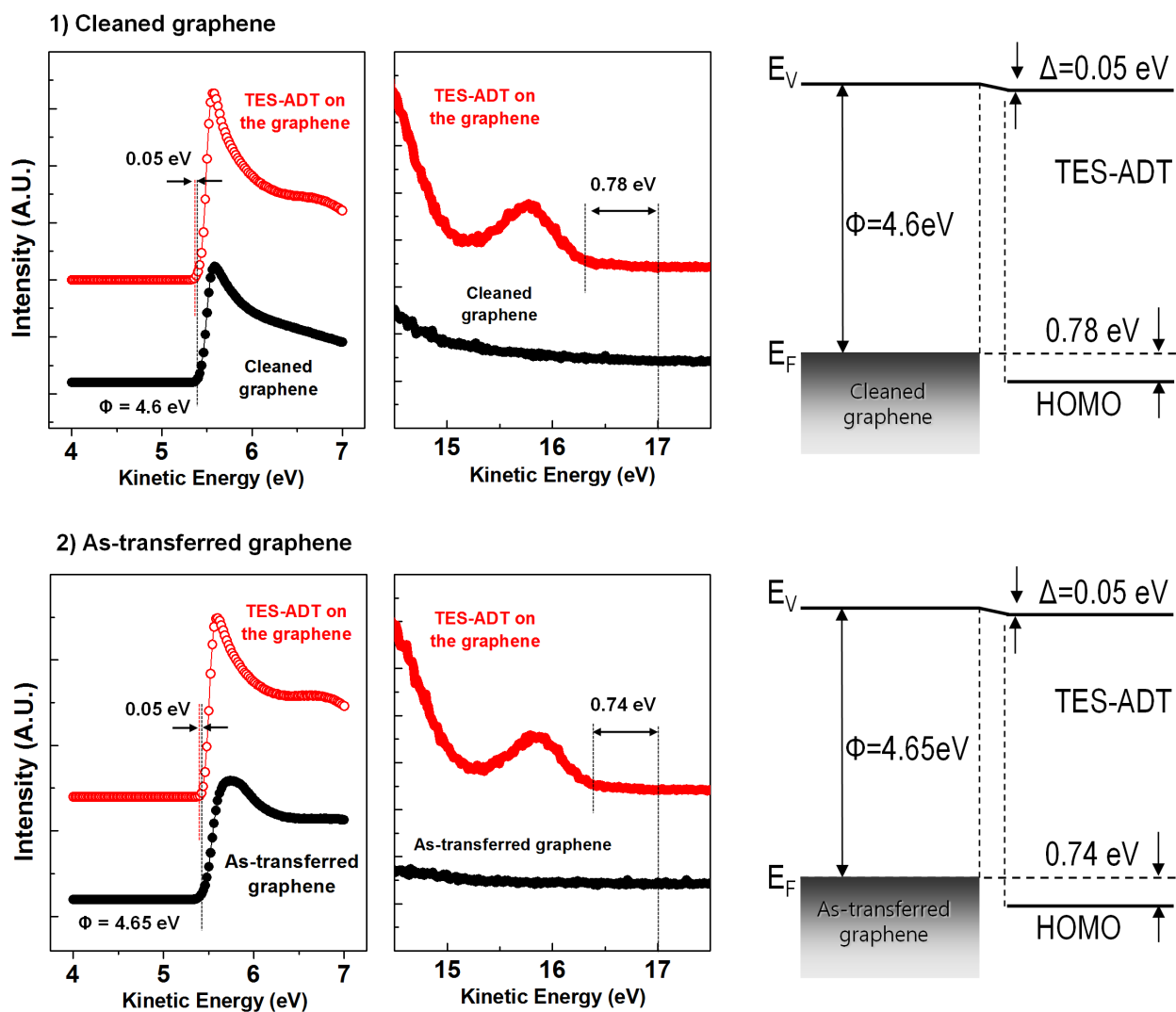


Fig. S10. UPS spectra of the secondary electron cutoff (left) and the valence band region (middle) for graphene electrodes and the solvent-vapor annealed TES-ADT thin-films on the graphene electrodes. Band diagrams of the TES-ADT on the cleaned/as-transferred graphene electrodes (right).

References

- ¹ S. B. Amor, G. Baud, M Jacquet, G. Nanse, P. Fioux, and M. Nardin, *Appl. Surf. Sci.* 2000, **153** (2-3), 172
- ² J. E. Lee, J. Ahn, J. Shim, Y. S. Lee, and S. Ryu, *Nat. Comm.* 2012, **3**, 1024.
- ³ M. M. Payne, S. R. Parkin, J. E. Anthony, C. C. Kuo, T. N. Jackson, *J. Am. Chem. Soc.* 2005, **127**, 4986.
- ⁴ S. Luan and G. W. Neudeck, *J. Appl. Phys.* 1992, **72**, 766